Status of CMB Observations

Martin Bucher
Université Paris 7/CNRS, Paris, France
and
University of KwaZulu-Natal, Durban, South Africa

24 August 2018, IAU General Assembly, Wien, Österreich

(With inputs from many colleagues. See credits at end.)

Talk Outline

1. Planck Legacy (focusing mainly on primordial aspects)
2. Current high-ℓ observations from the ground (largely exploring the so-called secondary anisotropies, of which we choose the kSZ as an example)
3. The Future: Searching for the CMB B-mode

2018 Planck Legacy Release

https://www.cosmos.esa.int/web/planck/publications

[See Gruber Lecture slides of Reno Mandolesi and Jean-Loup Puget from Tuesday for more details on Planck 2018 Results]

Discovery of the cosmic microwave ackground

1963 Penzias and Wilson (Bell Labs) observed a background of microwaves having a thermal spectrum with $T = 2.753K$. This temperature is (almost) the same no matter what the direction in the sky.

Theory – origin of the CMB anisotropy

Sachs-Wolfe formula

$$\frac{\delta T}{T}(\hat{\mathbf{n}}) = \left[\frac{1}{4}\delta_\gamma + \mathbf{v}_\gamma \cdot \mathbf{n} + \Phi\right]_i^f + 2\int_i^f d\eta \frac{\partial \Phi'}{\partial \eta}(\eta, \hat{\mathbf{n}}(\eta_0 - \eta))$$

$\Phi \equiv$ Newtonian gravitational potential (dimensionless)

δ_γ and $\mathbf{v}_\gamma$ describe the fractional density contrast and peculiar 3-velocity of of the photon component.

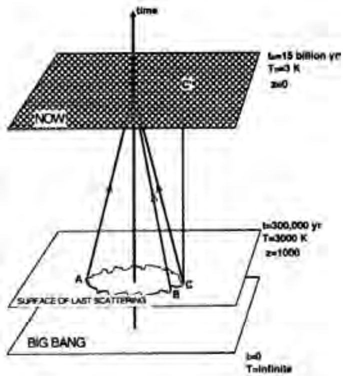

This treatment is somewhat naive because it assumes that the surface of last scatter is infinitely thin.

In reality the surface of last scatter has a width the smears the anisotropies on small scales.

The *Planck* mission

PLANCK Focal Plane

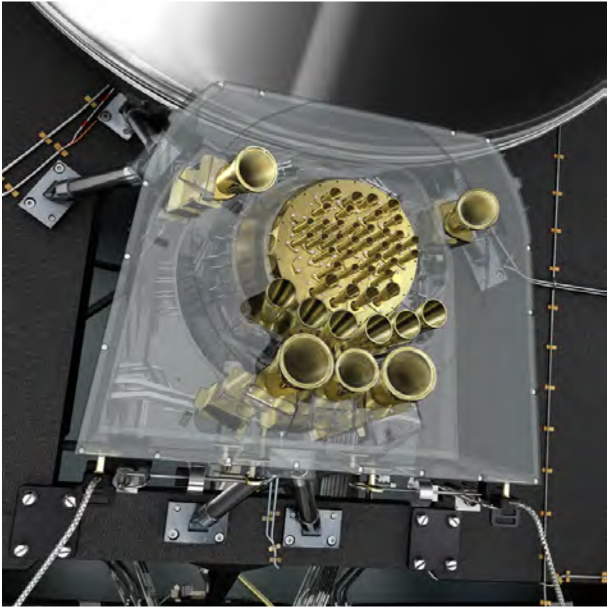

T & P Signals vs Frequency

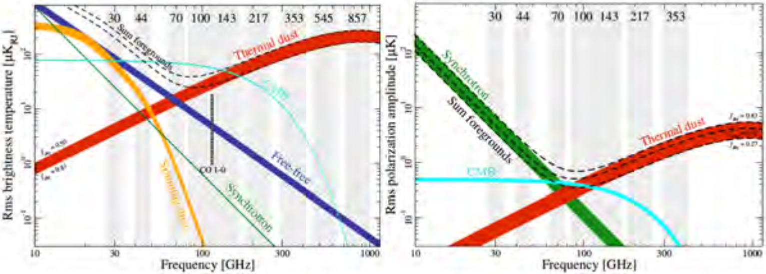

Fig. 4. Frequency dependence of the main components of the submillimetre sky in temperature (left) and polarization (right). The (vertical) grey bands show the *Planck* channels, with the coloured bands indicating the major signal and foreground components. For temperature the components are smoothed to 1° and the widths of the bands show the range for masks with 81–93 % sky coverage. For polarization the smoothing is 40′ and the range is 73–93 %. Note that for steep spectra, the *rms* shown here is dominated by the largest angular scales. But as shown by Fig. 5, on much smaller angular scales in regions far form the Galactic plane, the foreground signals fall far below the cosmological signal (except at the lowest ℓ, in polarization).

Planck Raw Temperature Maps

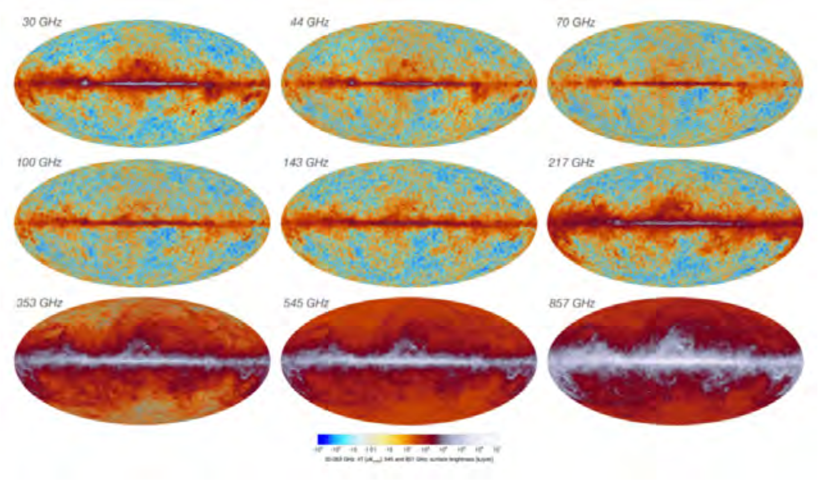

Planck Raw Polarization Maps

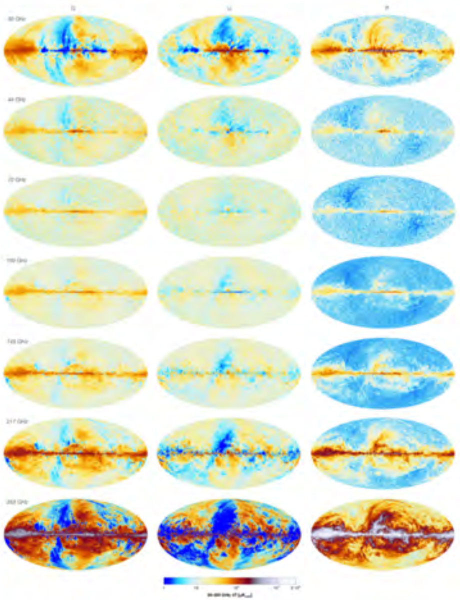

Cleaned Temperature Map

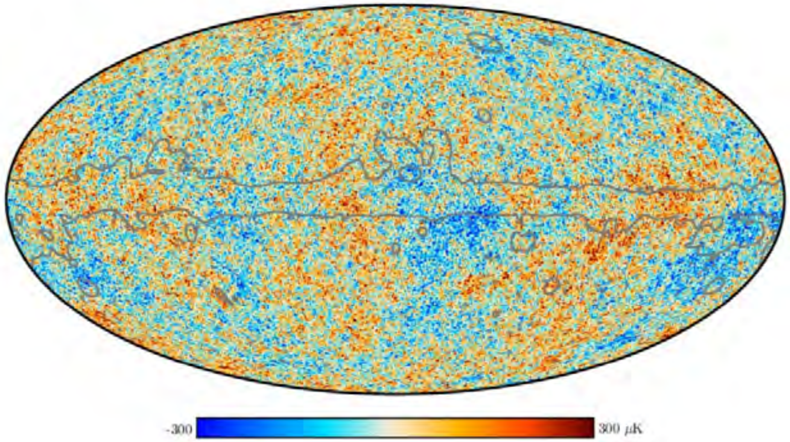

Cleaned Polarization Map

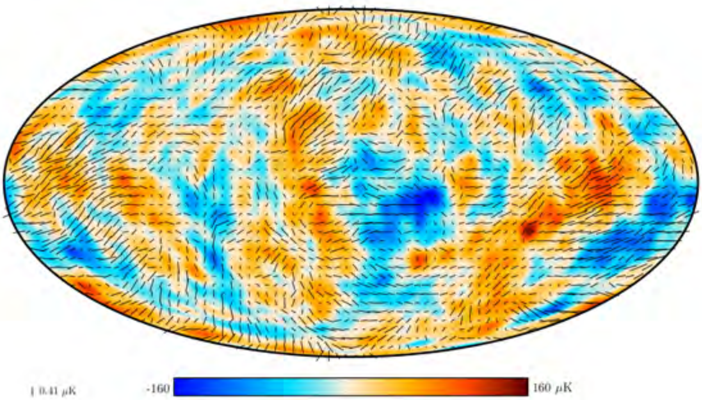

CMB Power Spectra: Current State of the Art

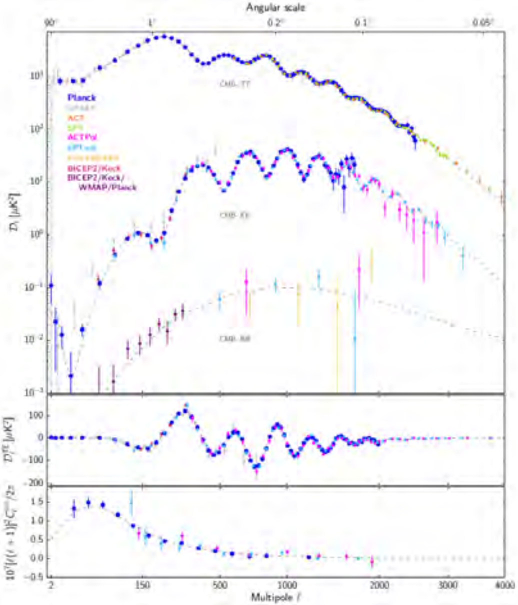

Parameters of the 6-Parameter Concordance Model

Parameter	Plik best fit	Plik [1]	CamSpec [2]	$([2]-[1])/\sigma_1$	Combined
$\Omega_b h^2$	0.022383	0.02237 ± 0.00015	0.02229 ± 0.00015	−0.5	0.02233 ± 0.00015
$\Omega_c h^2$	0.12011	0.1200 ± 0.0012	0.1197 ± 0.0012	−0.3	0.1198 ± 0.0012
$100\theta_{MC}$	1.040909	1.04092 ± 0.00031	1.04087 ± 0.00031	−0.2	1.04089 ± 0.00031
τ	0.0543	0.0544 ± 0.0073	$0.0536^{+0.0069}_{-0.0077}$	−0.1	0.0540 ± 0.0074
$\ln(10^{10} A_s)$	3.0448	3.044 ± 0.014	3.041 ± 0.015	−0.3	3.043 ± 0.014
n_s	0.96605	0.9649 ± 0.0042	0.9656 ± 0.0042	+0.2	0.9652 ± 0.0042
$\Omega_m h^2$	0.14314	0.1430 ± 0.0011	0.1426 ± 0.0011	−0.3	0.1428 ± 0.0011
H_0 [km s^{-1}Mpc^{-1}]	67.32	67.36 ± 0.54	67.39 ± 0.54	+0.1	67.37 ± 0.54
Ω_m	0.3158	0.3153 ± 0.0073	0.3142 ± 0.0074	−0.2	0.3147 ± 0.0074
Age [Gyr]	13.7971	13.797 ± 0.023	13.805 ± 0.023	+0.4	13.801 ± 0.024
σ_8	0.8120	0.8111 ± 0.0060	0.8091 ± 0.0060	−0.3	0.8101 ± 0.0061
$S_8 \equiv \sigma_8(\Omega_m/0.3)^{0.5}$	0.8331	0.832 ± 0.013	0.828 ± 0.013	−0.3	0.830 ± 0.013
z_{re}	7.68	7.67 ± 0.73	7.61 ± 0.75	−0.1	7.64 ± 0.74
$100\theta_*$	1.041085	1.04110 ± 0.00031	1.04106 ± 0.00031	−0.1	1.04108 ± 0.00031
r_{drag} [Mpc]	147.049	147.09 ± 0.26	147.26 ± 0.28	+0.6	147.18 ± 0.29

Planck 2018 TT With Residuals

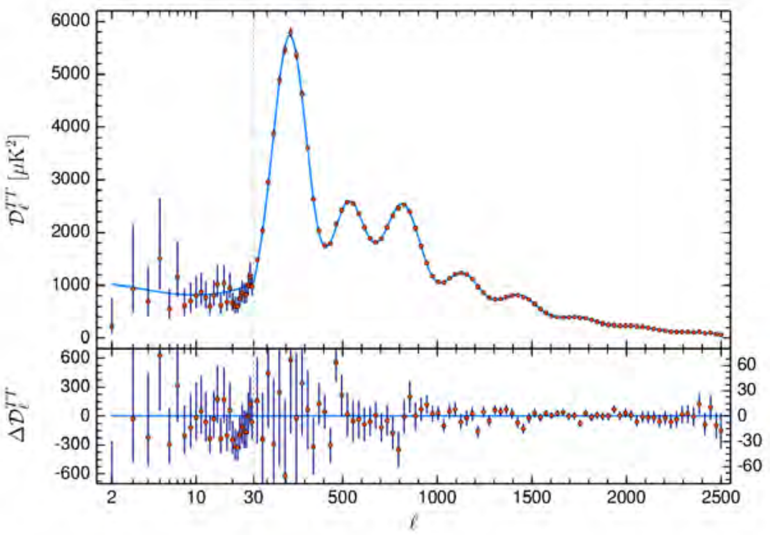

Planck 2018 TE and EE With Residuals

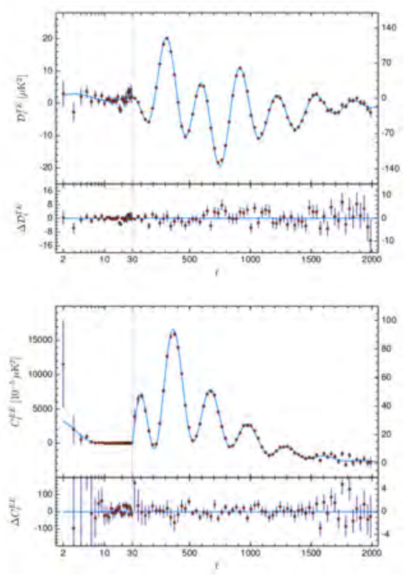

Evolution of Cosmological Parameters

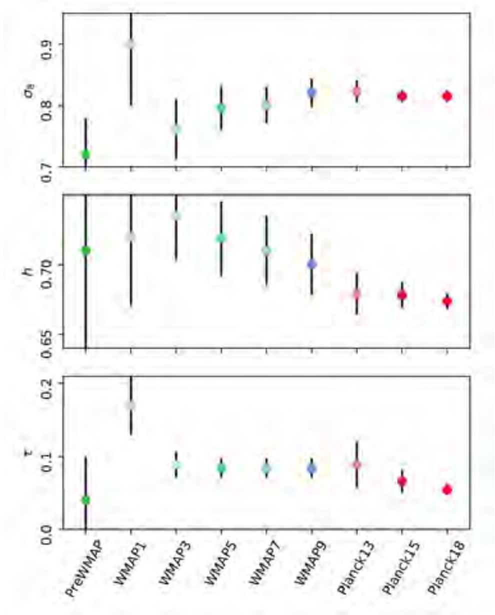

Tension with Conventional H Measurements

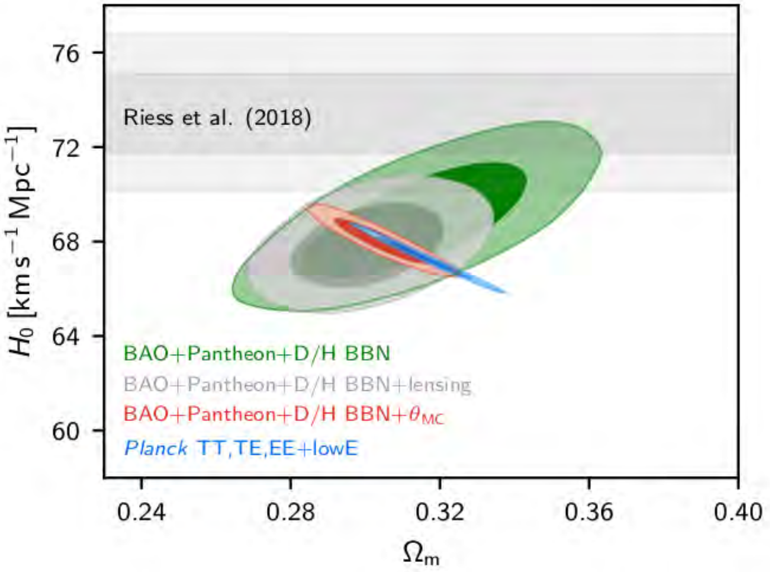

Inflationary Models: n_S-r Plane

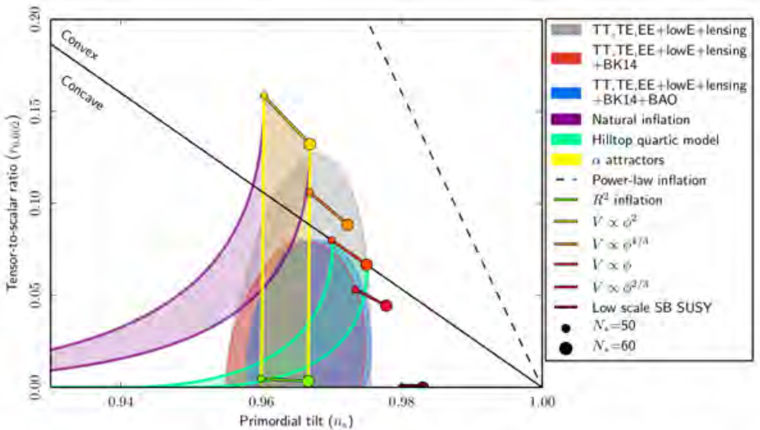

Fig. 23. Limits on the tensor-to-scalar ratio, $r_{0.002}$ as a function of n_S in the ΛCDM model at 95% CL, from *Planck* alone (grey area) or including BICEP2/Keck data 2014 (red) and BAO (blue). Constraints assume negligible running of the inflationary consistency relation and the lines show the predictions of a number of models as a function of the number of e-folds, N_*, till the end of inflation. This can be compared with the middle panel in the top row of Fig. 14 which gives a temporal perspective.

Concordance Scorecard

Prediction	Measurement
A spatially flat universe	$\Omega_K = 0.0007 \pm 0.0019$
with a *nearly* scale-invariant (red)	
spectrum of density perturbations,	$n_s = 0.967 \pm 0.004$
which is almost a power law,	$dn/d\ln k = -0.0042 \pm 0.0067$
dominated by scalar perturbations,	$r_{0.002} < 0.07$
which are Gaussian	$f_{NL} = 2.5 \pm 5.7$
and adiabatic,	$\alpha_{-1} = 0.00013 \pm 0.00037$
with negligible topological defects	$f < 0.01$

Secondary CMB Anisotropies

After subtraction of the CMB monpole and dipole, $\frac{\delta T}{T}$ for $\ell \lesssim 3000$ is dominated by the **primary** CMB anisotropies, which emanate from the **surface of last scatter** (i.e., almost at past intersection of our past light cone with the putative big bang singularity).
However, there are also other **secondary** anisotropies, which are imprinted as the photons propagate from the surface of last scatter to us today. [1] These include:

1. Gravitational Lensing of the CMB by intervening structures at intermediate redshift.
2. The Thermal Sunyaev-Zeldovich (tSZ) Effect
3. The Kinetic (or Kinematical) Sunyaev-Zeldovich (kSZ) Effect

[1] However, the integrated Sachs-Wolfe effect, the effect of rescattering by homogeneous reionization (i.e., τ) are conventionally regarded as being 'primary' anisotropies.

The Sunyaev-Zeldovich Effects

- Consider the rescattering of the CMB monopole by a cloud of possibly very hot reionized gas (e.g., from the diffuse ionized gas in a cluster).
- If the cloud had no peculiar motion (w.r.t. the Hubble flow) and if the electron gas temperature is exactly equal to the CMB temperature, the net effect is null, as if the cloud were not there.
- But,
  - kSZ: If the cloud is moving w.r.t. the local CMB rest frame, a dipole contribution
$$\frac{\delta T}{T_0}_{kSZ} = \frac{\tau}{c}(\hat{\mathbf{n}} \cdot \mathbf{v})$$
    is superimposed on the primary anisotropies, also with a perturbed blackbody frequency spectrum.
  - tSZ: If the cloud is hot $T \gg T_{CMB}$, a spectral distortion of the form
$$\left(\frac{\delta T(\nu)}{T_0}\right)_{tSZ} = \frac{\tau}{m_e c^2} F(x) = \delta y \; F(x)$$
    where $x = \nu/\nu_{CMB}$, $\nu_{CMB} = k_B T/h$, and
$$F(x) = \frac{x(e^x + 1)}{e^x - 1} - 4$$
    is superimposed.

kSZ and Peculiar Velocities

The kSZ effect is notoriously hard to measure because:

1. Unlike the tSZ effect, the kSZ has *precisely the same frequency dependence* as the primary CMB anisotropies (i.e., that of a perturbed blackbody).
2. It is **much smaller** in magnitude than the primary CMB anisotropies.

Therefore, the easiest and best way to detect kSZ is through **cross-correlations**.

In other words, one makes a prediction for δT_{kSZ} (using data from 3d galaxy surveys possibly combined with tSZ data) and then cross correlates this template with a properly filtered and cleaned map of $\delta T^{sky}_{blackbody}$. [This is how gravitational lensing of the CMB was first discovered, although now CMB lensing is measured directly, without resorting to cross-correlations.]

kSZ: A unique probe of peculiar velocities to arbitrarily high z

- Competing probes of peculiar velocities (i.e., using "standard candles") have errors that increase with z and thus are useful only within a small sphere in our immediate vicinity.
- kSZ peculiar velocities instead measure velocities relative to the local CMB rest frame (in which the CMB dipole about the object vanishes). [This is not a perfect reference but better than any other empirical cosmic rest frame.] Thus the errors are roughly independent of z. Thus we can probe peculiar velocities almost anywhere within our causal horizon.

Current status of kSZ observations

There are two basic strategies:

1. Select two massive collapsed objects that should be falling toward each other and predict $\delta T(1) - \delta T(2)$ including its sign, which is random for the noise from the primary CMB anisotropies. Challenge is to filter out the primary CMB signal and also the contamination from kSZ. Use stacking to accumulate S/N.
2. Reconstruct the entire proper velocity field $\mathbf{v}(\mathbf{x})$ to make a template for the expected $\delta T(\hat{\mathbf{n}})$ and cross-correlate with $\delta T^{sky}_{blackbody}(\hat{\mathbf{n}})$ with the statistic
$$\left\langle \delta T(\hat{\mathbf{n}})\ \delta T^{sky}_{blackbody}(\hat{\mathbf{n}}) \right\rangle .$$

Whereas the *tSZ* signal is dominated by highly collapsed objects (where the gas is especially hot) and roughly probes gas pressure along the line of sight, the kSZ probes the peculiar velocity field of the gas everywhere as long as it is ionized, or gas momentum averaged and projected along the line of sight.

Here we have emphasized proper velocity field, but the baryon density as well as the ionization fraction enters into determining the signal. Thus given a knowledge of the peculiar velocity field, we can probe where the ionized gas is situated.

First detection of kSZ

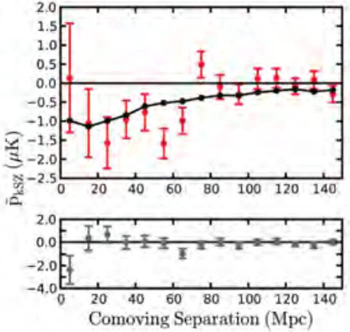

FIG. 1: The upper panel shows the mean pairwise momentum estimator, Eq. (4), for the 5000 most luminous BOSS DR9 galaxies within the ACT sky region (red points), with bootstrap errors. The solid line is derived from numerical kSZ simulations [31] using a halo mass cutoff of $M_{200} = 4.1 \times 10^{13} M_\odot$. The probability of the data given a null signal is 2.0×10^{-3} including bin covariances. The lower panel displays the same sum but with randomized map positions, and is consistent with a null signal.

Nick Hand et al. (ACT Collaboration), "Evidence of Galaxy Cluster Motions with the Kinematic Sunyaev-Zeldovich Effect," Phys. Rev. Lett. 109 (2012) 041101 ($\approx 2.9\sigma$ detection)

$$\tilde{p}_{\rm pair}(r) = \frac{\sum_{i<j} (\mathbf{p}_i \cdot \hat{\mathbf{r}}_i - \mathbf{p}_j \cdot \hat{\mathbf{r}}_j) c_{ij}}{\sum_{i<j} c_{ij}^2}$$

$$c_{ij} \equiv \hat{\mathbf{r}}_{ij} \cdot \frac{\hat{\mathbf{r}}_i + \hat{\mathbf{r}}_j}{2} = \frac{(r_i - r_j)(1 + \cos\theta)}{2\sqrt{r_i^2 + r_j^2 - 2 r_i r_j \cos\theta}},$$

$$\tilde{p}_{\rm kSZ}(r) = -\frac{\sum_{i<j} [(T_i - \mathcal{T}(z_i)) - (T_j - \mathcal{T}(z_j))] c_{ij}}{\sum_{i<j} c_{ij}^2}.$$

Another example

Planck Collaboration: P. A. R. Ade et al., Planck intermediate results XXXVII. Evidence of unbound gas from the kinetic Sunyaev-Zeldovich effect A&A 586, A140 (2016)

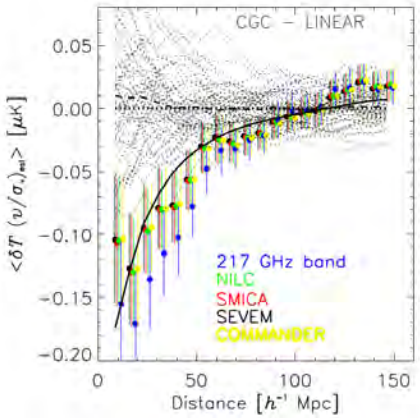

Many other papers (e.g., SPT & DES,...)

kSZ: The Future (Toward the CMB Stage-4 Experiment)

- Since galaxy clusters are small, kSZ studies are ideally performed by mapping the microwave sky from the ground, where telescopes of diameter $6 - 10$ m can be deployed at a reasonable cost.
- The high resolution maps, for example from ACT and SPT, are sufficient for a proof of concept, but there is much scope for improvement in (1) the sensitivity of the maps, (2) fraction of sky covered, and (3) better frequency coverage (in order to remove kSZ as well as the more conventional foregrounds).
- Likewise, because of the importance of cross-correlations, more extensive and deeper 3d galaxy surveys promise to improve on what is currently possible.

E and B Mode Polarization

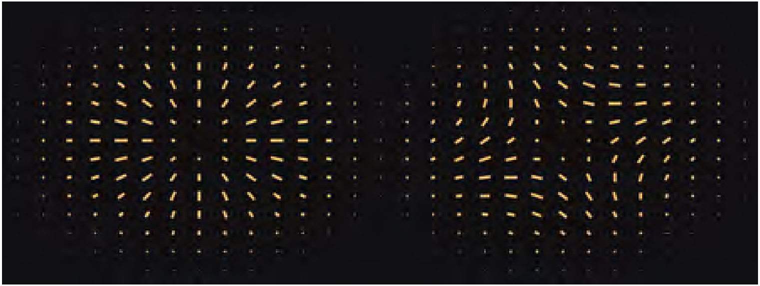

E mode   B mode

$$\mathbf{Y}^{(E)}_{\ell m,ab} = \sqrt{\frac{2}{(\ell-1)\ell(\ell+1)(\ell+2)}}\left[\nabla_a\nabla_b - \frac{1}{2}\delta_{ab}\nabla^2\right]Y_{\ell m}(\hat{\Omega})$$

$$\mathbf{Y}^{(B)}_{\ell m,ab} = \sqrt{\frac{2}{(\ell-1)\ell(\ell+1)(\ell+2)}}\frac{1}{2}\left[\epsilon_{ac}\nabla_c\nabla_b + \nabla_a\epsilon_{bc}\nabla_c\right]Y_{\ell m}(\hat{\Omega})$$

Modern CMB instrument: POLARBEAR as an example

Site:
Atacama, Chile

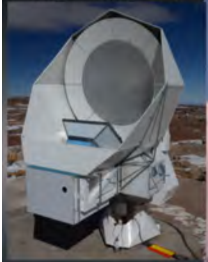

TES
bolometer
array

(UC Berkeley)

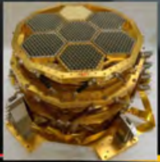

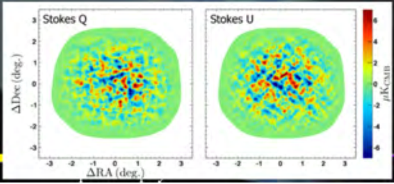

CMB power spectra

2017

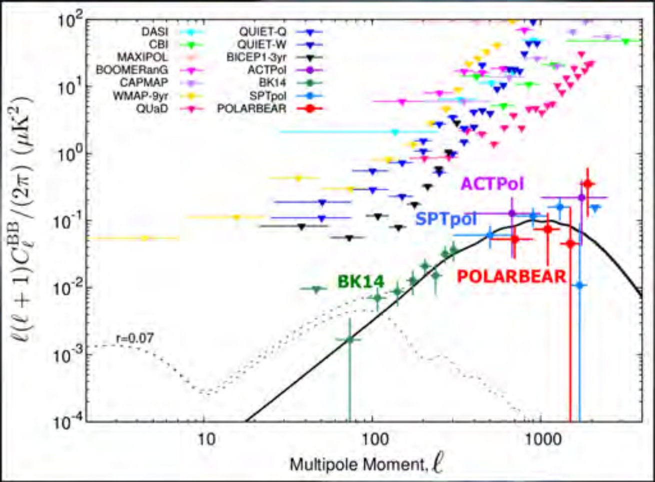

Y. Chinone
(UC Berkeley)

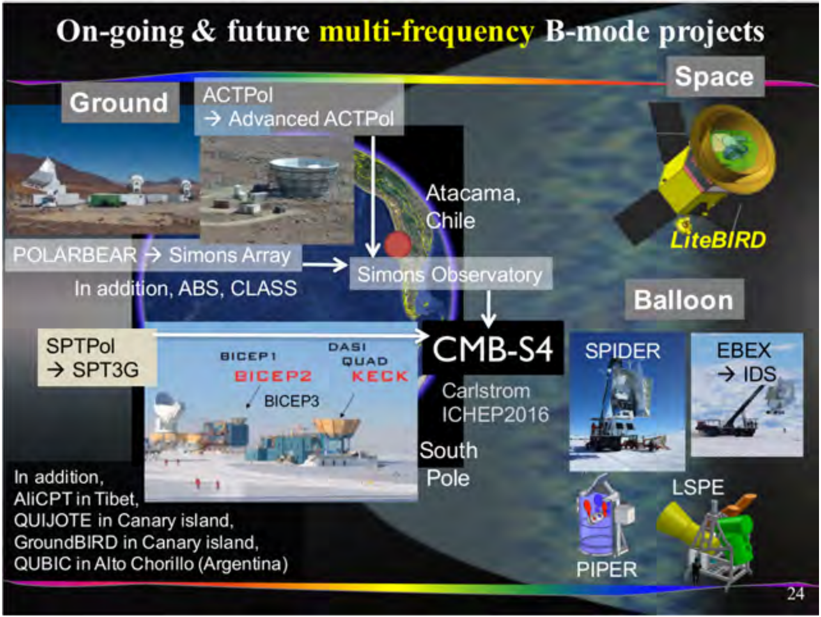
On-going & future multi-frequency B-mode projects
Ground
ACTPol
→ Advanced ACTPol
Atacama,
Chile
POLARBEAR → Simons Array
Simons Observatory
In addition, ABS, CLASS
SPTPol
→ SPT3G
BICEP1
DASI
QUAD
BICEP2
KECK
BICEP3
CMB-S4
Carlstrom
ICHEP2016
South
Pole
In addition,
AliCPT in Tibet,
QUIJOTE in Canary island,
GroundBIRD in Canary island,
QUBIC in Alto Chorillo (Argentina)
Space
LiteBIRD
Balloon
SPIDER
EBEX
→ IDS
LSPE
PIPER
24

Simons Observatory

Full operations in 2021

SIMONS OBSERVATORY

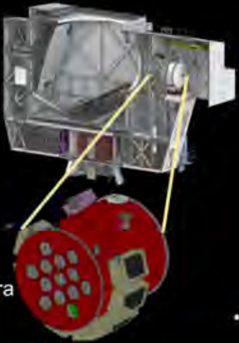

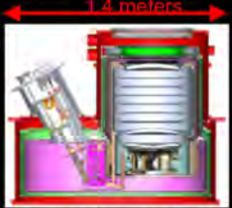

- Three telescopes each with a 50 cm aperture.
- A total of 30,000 detectors

- 6 meter off-axis Cross Dragone design
- 9 degree field of view – 9 times the throughput of ACT
- 1.7 arcmin resolution at 150 GHz
- Up to 70,000 detectors can be accommodated (30,000 planned)

- Extensive site infrastructure in Chile
- Data pipeline and analysis development

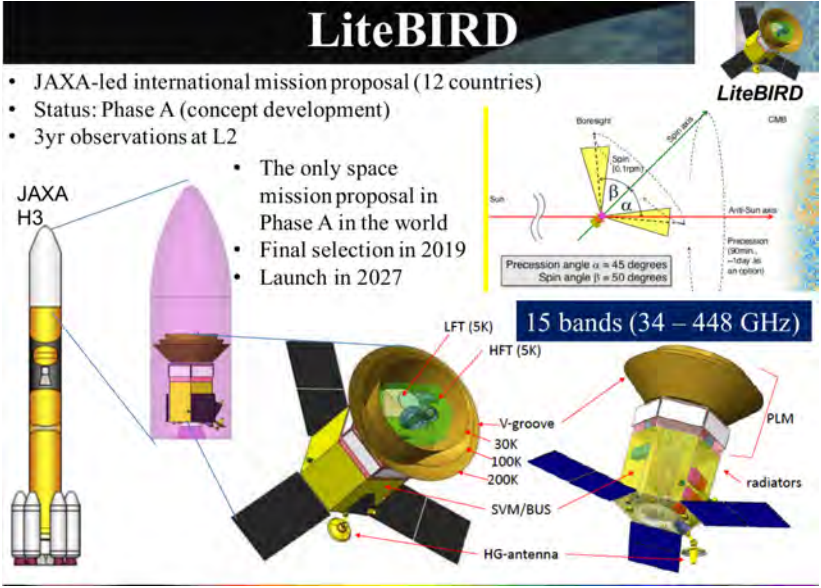
LiteBIRD
JAXA-led international mission proposal (12 countries)
Status: Phase A (concept development)
3yr observations at L2
The only space mission proposal in Phase A in the world
Final selection in 2019
Launch in 2027
JAXA H3
LiteBIRD
Boresight
Spin axis
Spin
Sun
Anti-Sun axis
CMB
Precession angle α = 45 degrees
Spin angle β = 50 degrees
15 bands (34 – 448 GHz)
LFT (5K)
HFT (5K)
V-groove
30K
100K
200K
SVM/BUS
HG-antenna
PLM
radiators

LiteBIRD expectation

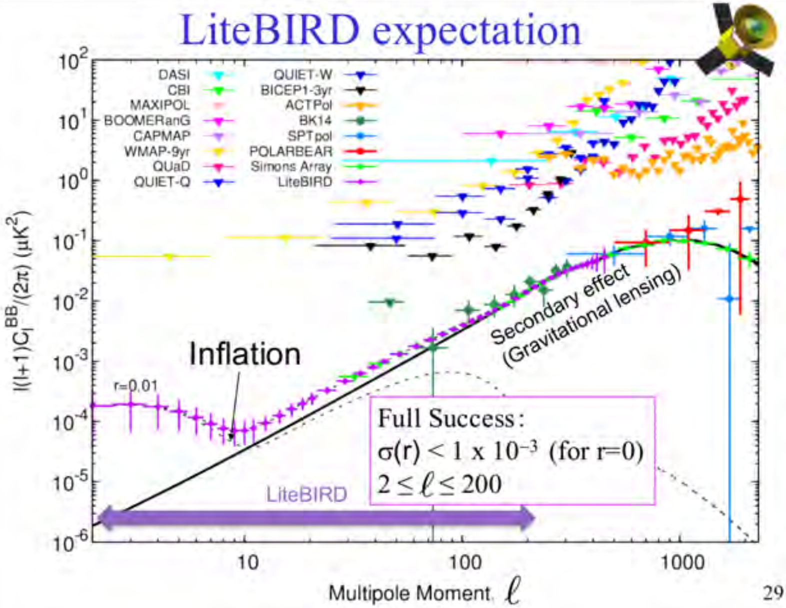

Impacts of discovery

LiteBIRD

- Direct evidence for cosmic inflation
  - Many models predict $0.003 < r < 0.05$
  - Narrowing down models in r vs. n_s plane
- Shed light on GUT-scale physics

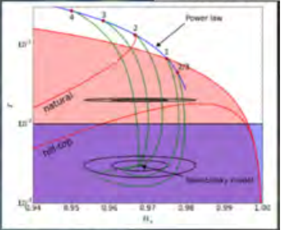

$$V^{1/4} = 1.04 \times 10^{16} \times \left(\frac{r}{0.01}\right)^{1/4} [GeV]$$

- New era of physics w/ experimental tests of QG
  - First observation of quantum fluctuation of space-time
  - Studies on top-down constraints in string theory in progress
    - $r > 0.01$ not easy (super-Planckian field excursions)
- Sense of wonder beyond science!

Future prospects on neutrinos

- CMB lensing B-mode
- BAO

Chance to resolve hierarchy independently of oscillation experiments

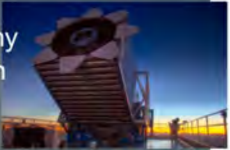

CMB-S4 Next Generation CMB Experiment in 2020s

N_{eff}	$Sum(m_\nu)$
3.046	> 59meV
$\sigma(N_{eff})$	$\sigma(\Sigma m_\nu)$
	Boss BAO prior
0.14	0.15eV
	Boss BAO prior
0.06	0.06eV
	DESI BAO $+\tau_e$ prior
0.027	**0.015eV**

τ(optical depth) and neutrino mass

- Better E-mode measurement for $\ell < 20$ improves τ
- Better τ improves Σm_ν by resolving degeneracies

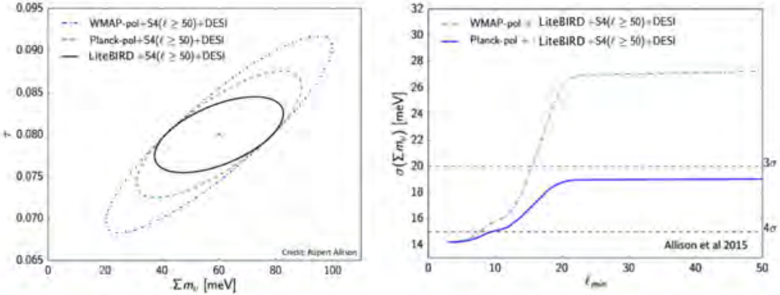

Low ℓ measurements (e.g. LiteBIRD) contribute to Σm_ν!

CMB-S4 Goal #1 - **Search for primordial gravitational waves via their "B-mode" polarization signature**

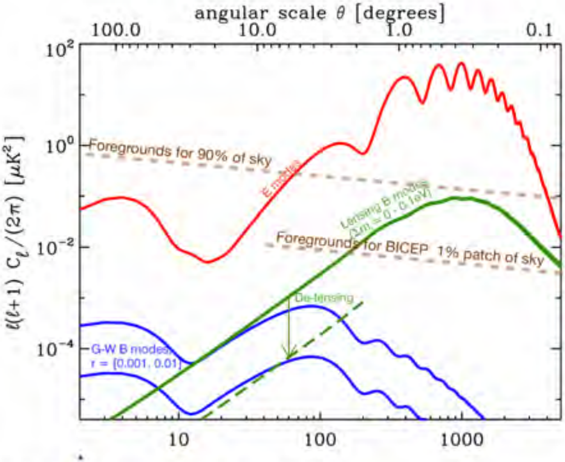

Challenges:

- Sensitivity,
- Galactic foregrounds,
- Lensing B-modes

CMB-S4 Survey:

- ~3-8% of sky
- 0.5m telescopes +
- 5m telescope for delensing
- ~1uK-arcmin depth

Figure from J. Carlstrom/T. Crawford.

CMB S4 to deploy 10^{5-6} detectors from the ground

Foregrounds =>

Observing bands from 20GHz to 270GHz, to subtract out Galactic Dust and Synchrotron emission by a factor of ~10.

Source: CDT Report (2017)

		Band center in GHz									
		20	30	40	85	95	145	155	220	270	N_det total
5m telescopes (2-3)											
Beam fwhm	arcmin	11	7	5.2	-	2.2	1.4	-	1	0.8	
Number of detectors		420	890	1,600		75,000	75,000		25,700	25,700	204,310
0.5m telescopes (~14)											
Beam fwhm	arcmin	-	77	58	27	24	16	15	11	8.5	
Number of detectors			260	470	17,000	21,000	18,000	21,000	34,000	54,000	165,730

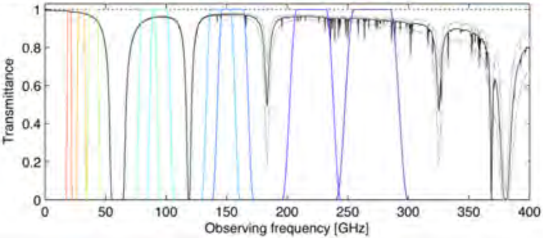

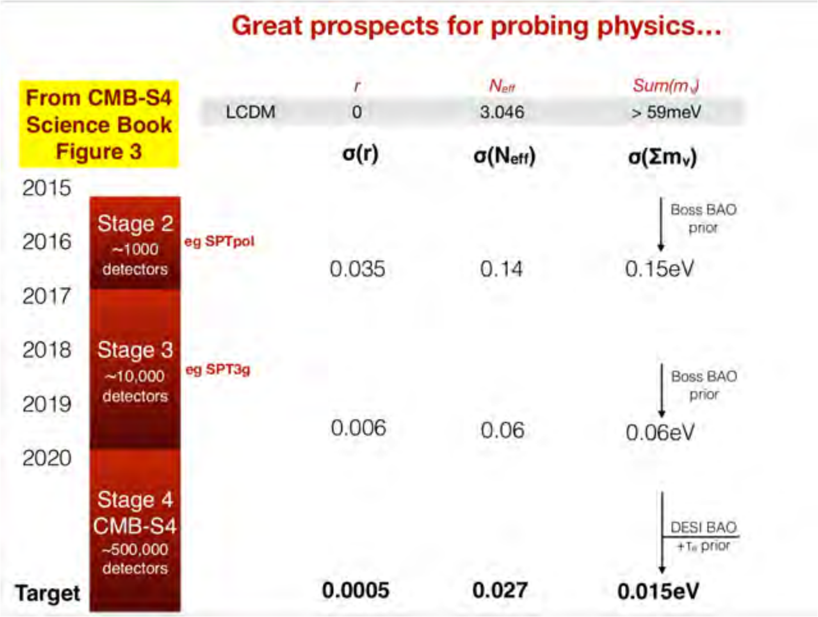
Great prospects for probing physics...
From CMB-S4 Science Book Figure 3
r
N_eff
Sum(m_ν)
LCDM
0
3.046
> 59meV
σ(r)
σ(N_eff)
σ(Σm_ν)
2015
2016
2017
2018
2019
2020
Target
Stage 2
~1000 detectors
eg SPTpol
Stage 3
~10,000 detectors
eg SPT3g
Stage 4
CMB-S4
~500,000 detectors
Boss BAO prior
0.035
0.14
0.15eV
Boss BAO prior
0.006
0.06
0.06eV
DESI BAO +τ prior
0.0005
0.027
0.015eV

Conclusions:

1. We have come a long way since the 1965 Penzias and Wilson discovery and the 1992 COBE DMR CMB anisotropy first detection.
2. The state of the art today is the result of experience amassed through many experiments from space and from the ground. From space there is COBE, WMAP, and Planck, and from the ground dozens of experiments culminating in ACT, SPT, BICEP, POLARBEAR,...... [see previous slides]
3. The ESA Planck Mission has exhausted virtually all the statistically exploitable information from the primordial CMB temperature anisotropies on large and intermediate angular scales. **But substantial scope remains for improvement in the polarization measurements on all angular scales, as well as the temperature anisotropy on small angular scales.**
4. Ground-based microwave observations are ideally suited to mapping the small-scale anisotropies, for example for determining the absolute neutrino masses, mapping the hot gas and the peculiar velocities, and the gravitational lensing spectrum.
5. Space is ideally suited to mapping the large-angle B modes for discovering primordial gravitational waves from inflation, determining the reionization optical depth τ at the cosmic variance limit (crucial to the maximal scientific exploitation of many surveys [e.g., Euclid, LSST,.....]). Space provides an exquisitely stable environment able to access frequencies inaccessible through the atmosphere.
6. CMB observations have become harder, but the rewards in terms of science return remain tremendous. An exciting future remains for this field.

Credits

Special thanks to: The Planck Collaboration, Jamie Bock, Yuji Chinone, Mark Devlin, Olivier Dore, Jean-Christophe Hamilton, Shaul Hanany, Chao-Lin Kuo, Si-yu Li, Hitoshi Murayama, Jean loup Puget, Rafael Rebolo, Shun Saito, Osamu Tajima, Masahiro Takada, Jan Tauber, and especially Masashi Hazumi for inputs.

[See poster contribution of Tadayasu Dotani, *Concept study of the LiteBIRD satellite for CMB B-mode polarization*, Divion J poster session for more details on one of the space options.]

A more complete listing of future experiments will be provided in the proceedings.